Development and Verification of a µN Thrust Balance for High Voltage Electric Propulsion Systems

B. Seifert[1], A. Reissner[2], N. Buldrini[3] and F. Plesescu[4]
FOTEC Forschungs- und Technologietransfer GmbH, Wr. Neustadt, Austria

C. Scharlemann[5]
University of Applied Sciences Wr. Neustadt, Austria

In the scope of the development of the µPPT and the mN-FEEP thruster, a µN thrust balance has been developed, suitable for thrust measurements of high voltage electric propulsion systems. The system comprises a horizontal beam which is suspended by two spring bearings. Its displacement is measured using a high-precision optical distance transducer. The balance features a measurement range from few µN to several mN and can utilize a propulsion system with a total weight of up to 13 kg. To account for the low damping of the beam which under vacuum is only caused by friction of the utilized spring bearings, a passive magnetic eddy current brake has been implemented to reduce measurement noise and oscillations caused by over- or undershoot. An axial liquid metal contact system has been developed in order to minimize the influence of electrical connections. This enables the thruster to be supplied with various voltages – even high voltage and high current can be utilized without degradation of thrust measurement sensitivity. This paper gives a detailed description of the design, the achievable measurement accuracy, the calibration process and an outlook for further developments and improvements.

Nomenclature

I_{sp}	=	specific impulse, s
T	=	periodicity, s
J, J´	=	momentum of inertia, kg m^2
F, F_0, F_a	=	force, N
k, k´	=	spring rate of bearings, Nm/rad
p	=	impulse, Ns
r, r_a	=	distance to pivot, m
x	=	deflection, m
α	=	thruster misalignment, rad
τ	=	torque, Nm
ω_0, ω	=	angular frequency, Hz
θ	=	deflection angle, rad
η	=	duty cycle

[1] Senior Scientist, Aerospace Engineering, seifert@fotec.at
[2] Head of Department, Aerospace Engineering, reissner@fotec.at
[3] Research Scientist, Aerospace Engineering, buldrini@fotec.at
[4] Lead Technician, Aerospace Engineering, plesescu@fotec.at
[5] Head of Department, Aerospace Engineering, carsten.scharlemann@fhwn.ac.at

I. Introduction

In order to determine the generated thrust of field-emission electric propulsion (FEEP) or of miniaturized pulsed plasma thruster (µPPT) systems which are being manufactured and tested at FOTEC (former Department of Advanced Space Propulsion, AIT), a torsion-based µN thrust balance has been developed [1, 2, 3, 4, 5]. The system comprises a horizontal Aluminum beam at the length of 70 cm whose center is suspended by two stainless steel spring bearings type G10 ½" manufactured by C-Flex with the nominal spring rate of 0.096 Nm/rad. A monolithic stainless steel holder is retaining them ensuring low thermal drift, high reproducibility and ultra-low noise levels. The thrust balance is equipped with two tables which are positioned at both ends of the beam (see Fig. 1). The thruster which is to be characterized is mounted on one of them and a counter weight with the same mass is mounted on the other one. This ensures the cancellation of the overall torque and prevents the bearings from absorbing shear forces. The total capacity of the thrust balance is 13 kg on each table.

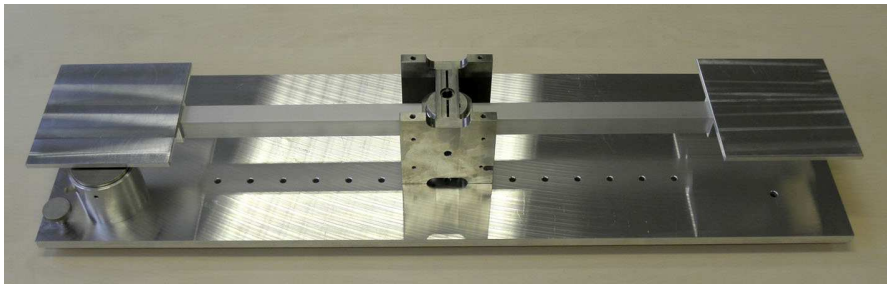

Fig. 1 µN Torsion thrust balance developed at FOTEC.

When a thrust is generated by the propulsion system, the beam of the balance is deflected. An optical reflection ratio-based displacement transducer mDMS-D64 manufactured by Philtec is being utilized to determine deflection and thus the force. With the maximum deflection of ±3.0 mm the thrust range of up to ±6.8 mN is covered. Since electric propulsion thruster operation is required to be performed in high-vacuum conditions, there is no damping of the system due to air friction. It is therefore required to install a damping system in order to avoid long-lasting oscillations. The FOTEC µN thrust balance utilizes an eddy current brake with a strong neodymium permanent magnet. Due to the relative movement of the Aluminum table the induced currents tend to slow down it down.

Depending on the load the momentum of inertia is changing which in turn affects the response time of the system. It might therefore not be possible to resolve the thrust pulse generated by non-continuous propulsion systems like pulsed plasma thrusters [6]. The response time dependency of the thruster weight is treated in next section. For the characterization of FEEP (see Fig. 2) emitters with constant thrust the low response rate can be accepted in general.

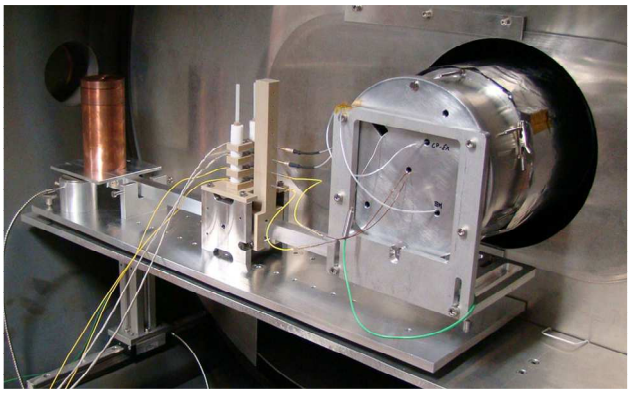

Fig. 2 µN Torsion thrust balance with mounted mN FEEP thruster at FOTEC vacuum test facility.

II. Operation of pulsed Thrusters

In particular when pulsed thrusters are to be characterized with the FOTEC µN thrust balance a low response time would be required to be able to resolve the generated thrust pulses. The pulse duration of common pulsed plasma thrusters is in the order of µs which cannot be acquired properly by most force measurement systems [7, 8]. An averaging effect of the generated thrust comparable with a low-pass filter with the cut-off frequency at the eigen-frequency occurs and only the average thrust can be quantified, but not the peak thrust level or the pulse duration.

For sake of simplify we assume a propulsion system which generates a rectangular pulse train with periodicity T. With the duty cycle η the pulse duration is ηT and the nominal thrust level is $\boldsymbol{F}_0$. The following expression defines the thrust

$$\boldsymbol{F}(t) = \begin{cases} \boldsymbol{F}_0 & t \equiv T < \eta T \\ 0 & t \equiv T \geq \eta T \end{cases}. \tag{1}$$

The thruster is mounted at the distance $\boldsymbol{r}$ with respect to the pivot and the torque $\boldsymbol{\tau}(t) = \boldsymbol{r} \times \boldsymbol{F}(t)$ is transferred to the balance. For the thruster orientation perpendicular to the beam of the balance and using $F(t) = |\boldsymbol{F}(t)|$ and $r = |\boldsymbol{r}|$ the torque is maximal and equals to $\tau(t) = r\,F(t)$. The displacement of the beam denoted by angle $\theta(t)$ is described by the inhomogeneous second-order differential equation

$$J\,\ddot{\theta}(t) + c\,\dot{\theta}(t) + k\,\theta(t) = \tau(t) \tag{2}$$

with the momentum of inertia J of the movable parts including beam and tables, the rotational friction c caused by the damping system and the spring rate k of the bearings. At first eq. (2) is only considered for $t < \eta T$ and the force $F(t)$ resolves to F_0 with the constant torque $r\,F_0$. The general solution is therefore

$$\theta(t) = \frac{r\,F_0}{\kappa} + \alpha\, e^{-\frac{c}{2J}t + i\,\omega t} + \beta\, e^{-\frac{c}{2J}t - i\,\omega t} \quad \text{with} \quad \omega = \sqrt{\frac{k}{J} - \frac{c^2}{4J^2}}\,. \tag{3}$$

With the initial conditions $\theta(0) = 0$ and $\dot{\theta}(0) = 0$ the arbitrary coefficients α and β of eq. (3) can be determined and the deflection angle results in

$$\theta(t < \eta T) = \frac{r\,F_0}{k}\left(1 - e^{-\frac{c}{2J}t}\left(\cos\omega t + \frac{c}{2J\,\omega}\sin\omega t\right)\right). \tag{4}$$

If the pulses of the thruster are short compared to the periodicity $\eta \ll 1$ eq. (4) at time ηT resolves to

$$\theta(t = \eta T) \to 0 \text{ and } \dot{\theta}(t = \eta T) \to \frac{r\,F_0\,\eta T}{J} = \frac{r\,p}{J} \tag{5}$$

with the defined impulse $p = F_0\,\eta T$ which is transferred to the beam of the balance periodically every time the thruster is fired. Eqs. (5) can now be utilized as initial conditions for eq. (3) to describe the deflection at the time $t > \eta T$ when $F(t)$ and thus the torque $\tau(t)$ vanish.

$$\theta(t > \eta T) = \frac{r\,p}{J\,\omega}\, e^{-\frac{c}{2J}(t - \eta T)} \sin\omega\,(t - \eta T) \tag{6}$$

This deflection angle has to be averaged over the period T and since linear differential equations can be superimposed, the pulses at the times $t = -T$ and $t = -2T$ and so on also contribute to the average deflection angle. With the assumption of eq. (5) this contributions can be summed up and result in

$$\bar{\theta} = \frac{1}{T}\sum_{i=0}^{\infty}\int_{(i+\eta)T}^{(i+1)T}\theta(t)\,\mathrm{d}t \to \frac{1}{T}\sum_{i=0}^{\infty}\int_{iT}^{(i+1)T}\theta(t)\,\mathrm{d}t = \frac{1}{T}\int_0^{\infty}\theta(t)\,\mathrm{d}t = \frac{r\,p}{T\,k}\,. \tag{7}$$

The impulse can now be deduced from the deflection angle measurement

$$p = \frac{T\,k}{r}\,\bar{\theta} \tag{8}$$

and consequently the average thrust results in

$$\bar{F} = \frac{p}{T} = \frac{k}{r}\,\bar{\theta} \tag{9}$$

which confirms the assumption that even when the response time of the thrust balance is much greater than the pulse duration of the thruster, the average thrust can be determined reliably. The only remaining restriction is the inability to resolve the pulse accurately in the time domain.

The optical displacement transducer is not able to directly determine the deflection angle but the change in distance between the sensor and the mirror mounted on the beam of the balance. The simple trigonometric relation

$$\tan\bar{\theta} = \frac{\bar{x}}{r} \rightarrow \bar{\theta} \tag{10}$$

can be approximated for small deflections $\bar{x} \ll r$ with the equal distance r from the pivot to the sensor like the thruster. The average force can now be rewritten as

$$\bar{F} = \frac{p}{T} = \frac{k}{r^2}\,\bar{x}\,. \tag{11}$$

It is obvious that in order to increase the sensitivity of the thrust measurement system the spring rate is required to be minimized and the distance from the pivot is to be maximized.

In Fig. 3 the response frequency for thruster weights of up to 13 kg is illustrated. Due to the contribution to the total momentum of inertia in particular at high thruster weights the response frequency drops to 0.05 Hz at the maximum allowable load.

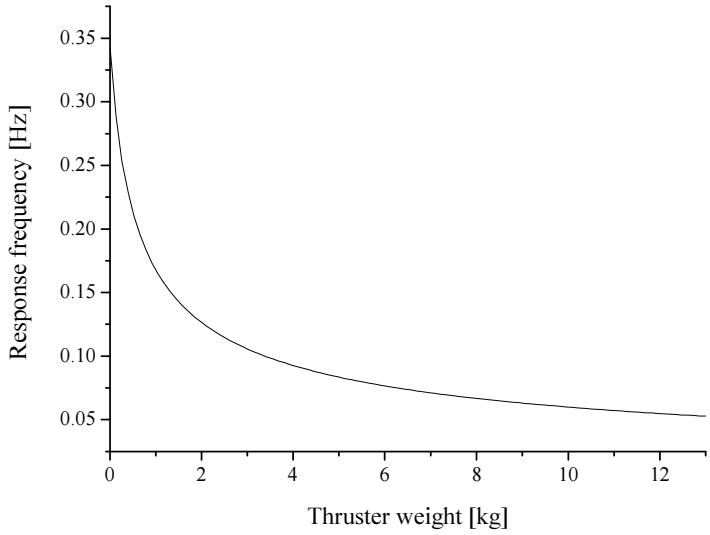

Fig. 3 Response frequency as a function of the thruster weight.

III. Electrical Feed-Throughs

Most thrusters require electrical connection to supply them with power, to enable or disable them, to set the thrust level or to monitor a variety of parameters like temperature or pressure. The common approach is the utilization of thin wires hanging from the top of the balance to the table where the thruster is mounted. Alternatively these wires can be guided through the spring bearings. Even if the tension of the wires does not significantly affect the spring rate of the system leading to a systematic error several other effects might corrupt the accuracy of the measurement.

If the isolation of the cable is made of PVC, silicone or some other plastics the softener will volatilize gradually and in particular under vacuum conditions. Thus the spring rate cannot be assumed as being constant over time. In addition if the thin lines supply the thruster with power they tend to heat up at higher current ratings which in turn makes the isolator expand at a different rate than the copper strands. Consequently the cable will bend similarly to the bimetal effect and generate a phantom force.

In addition high currents generate a magnetic field around the wires which might interact with other wires, magnets or other ferric material in the immediate vicinity. Moreover the Earth magnetic field must not be neglected when ultra-precise measurements are to be performed. In particular FEEP thrusters are required to be operated at high voltages of up to 15 kV or more and the electrostatic forces between the wires or between a wire and the grounded vacuum chamber must not be underestimated.

These common effects and problems can drastically be reduced if a conductive liquid is utilized to connect the wires on the movable part of the balance with the electrical connections outside the test facility [9]. At low pressure ionic aquatic solutions tend to evaporate which would not only inhibit endurance tests but would contaminate the thruster and the vacuum chamber. The μN thrust balance developed at FOTEC therefore utilizes liquid metal contacts to ensure good electrical conductivity between the contacts. Apart from Mercury which is poisonous and carcinogenic only some alloys are in liquid state at room temperature. In this case Galinstan is the most eligible candidate. It consists of Gallium, Indium and Tin and since the FEEP thruster uses Indium as propellant and wires and connections are soldered with Tin, no remarkable contamination of the vacuum chamber is to be suspected.

Every contact consists of a PEEK bar which is mounted on the centered beam holder with a blind hole filled with Galinstan. A stainless steel pin from the side is contacting the liquid metal. Another pin which is fixed to the PEEK part mounted on the beam is dipping into the reservoir (see Fig. 4).

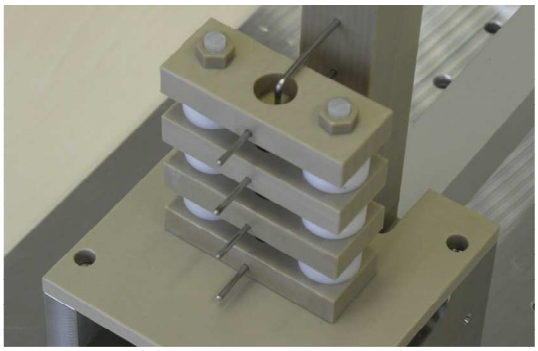

Fig. 4 Four electrical feed-throughs with Teflon isolators in between – reservoirs are to be yet filled.

Since every pin dipping into the liquid metal reservoir is exactly in line with the axis of rotation no relative movement occurs when the beam is excited. The pin only rotates within the reservoir and therefore does induce only marginal friction forces and no influence on the spring rate of bearings has been observed experimentally.

For multi-FEEP thruster tests the propellant needs to be liquefied at first and a heating power of more than 12 W at a typical current of 1 A is required. In one of the tests performed at FOTEC the current of 1 A has been applied to a contact pair but no deflection of the beam has been observed. The same null measurement has been acquired when

high voltage difference of 15 kV has been applied to two of the contacts. Due to the good conductivity of the stainless steel spring bearings the beam can be utilized as signal ground reference but it is recommended not to feed high currents through the bearings in order to avoid heating up and thus offset drifts or influences on the spring rate.

IV. Thrust Balance Calibration

The torsion thrust balance can only meaningfully be utilized when the ratio between the applied force and the acquired deflection of the beam has been determined before. In general there are two ways to calibrate the balance: a known force can be applied to measure the deflection or the balance is excited to perform free oscillations. Both methods are described in the next paragraphs.

Since the beam is excited horizontally it is not possible to place a calibrated mass on the balance. In the regime of µN to mN the utilization of pulleys or other mechanical systems is not advisable since friction or sticking forces might drastically affect measurement accuracy. A so called force actuator is typically used instead [10]. Electrostatic or magnetic forces are induced and applied to the moveable parts of the balance. When the force actuator has been calibrated before, the ratio between force and deflection can successfully be determined in this way. The detailed theory of operation of such a device and potential drawbacks and pitfalls during development or fabrication would go beyond the scope of this document but it should be noted that the accurate generation of a known force in the µN to mN range is a sophisticated task and no off-the-shelf solutions do exist to our knowledge that can be used for the force range and accuracy level required. In [11] additional calibration techniques utilizing the generation of electrostatic or gas dynamic forces are compared.

For the second method of calibration the thrust balance is operated as a torsion pendulum. Eq. (2) which describes the deflection angle over time can be simplified since the magnetic damping system is removed during calibration which results in $c = 0$. As pointed out the free oscillation is recorded (see Fig. 5) and thus no external torque $\tau(t) = 0$ is applied. Consequently eq. (2) is reduced to

$$J\,\ddot{\theta}(t) + k\,\theta(t) = 0. \tag{12}$$

The trivial solution of the equation is

$$\theta(t) = A \sin \omega_0 t \quad \text{with} \quad \omega_0 = \sqrt{\frac{k}{J}}\,. \tag{13}$$

The momentum of inertia J can analytically be calculated and with the measurement of the oscillation frequency ω_0 the spring rate

$$k = \omega_0^{\,2}\, J \tag{14}$$

can be computed. It is noticeable that the oscillation frequency ω_0 does not depend on the amplitude A which facilitates the determination of ω_0. The approximation $\omega_0 \sim \omega$ which is required for eq. (14) is only permitted if the damping factor of the system is low, thus $c \ll \sqrt{4\,k\,J}$ which is justified for free oscillation under vacuum in most applications.

In general the lower the oscillation frequency the better it can be measured since more samples can be acquired per period. It is therefore common practice to increase the momentum of inertia by adding test weights with known momentum of inertia to both tables. In addition spring bearings tend to change their rate depending on the axial load which suggests calibrating the balance at the same load as if the thruster was mounted. One of the test weights can be utilized as a counter weight for the thruster later on.

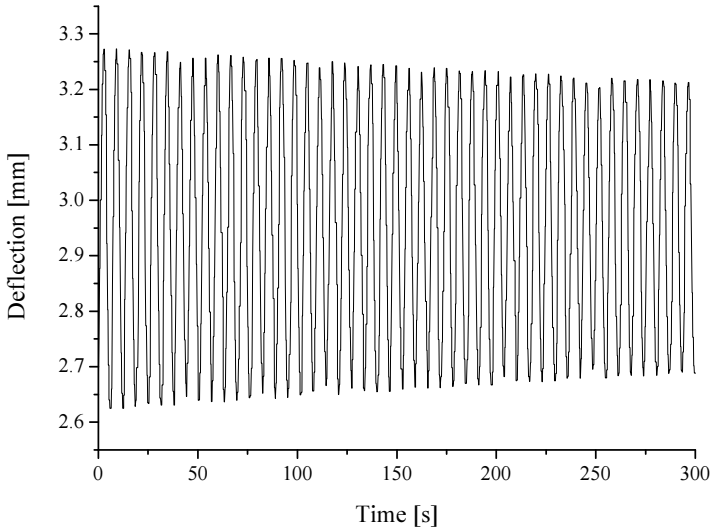

Fig. 5 Typical torsion pendulum oscillation at low damping rate.

V. Uncertainty Budget Calculation

For accurate thrust measurement not only the calibration of the balance is important but also the uncertainty of the measured value is required to be computed in order to allow the thrust measurement being compared with values determined at other thrust measurement facilities.

The uncertainty budget calculation below is setup for the thrust balance itself with test weights of 1.071 kg each. In addition ambient influences like vacuum pressure or temperature and other uncertainties like mounting accuracy of the thruster or optical displacement transducer accuracy are considered. All contributions to the total uncertainty budget are listed in Table 1 below.

Quantity	Unit	Description
δJ	Kg m^2	Total momentum of inertia including beam and mounted parts
δk	Nm/rad	Spring rate of bearings
δm	Nm/rad	Load influence on the spring rate
$\delta \omega$	Hz	Measurement of eigen-frequency during calibration
δd	N/s	Drift rate
δv	Nm/rad	Vacuum chamber pressure influence on the spring rate
δT	Nm/rad	Temperature influence on the spring rate
δx	m	Optical displacement transducer absolute accuracy
α	rad	Pointing inaccuracy of thruster mounting

Table 1 Contributions to uncertainty budget.

All these uncertainties influence the value of the spring rate. For the uncertainty budget calculation eq. (14) is utilized as the starting point. Apart from the oscillation frequency ω_0 the momentum of inertia and the corresponding uncertainties need to be calculated. Table 2 contains the parts that are relevant for that computation.

The beam length and the positioning accuracy of the tables and the test weights are assumed to be ±1.0 mm. If not noted otherwise all specified uncertainties have a coverage factor of 1.

Part	Value [kg m²]	Uncert. [kg m²]	Material	Remarks
Beam	0.008050	0.000069	Stainless steel	
Bearing Holder	0.000096	0.000001	Stainless steel	
Table 1	0.022324	0.000150	Aluminum	
Table 2	0.022324	0.000150	Aluminum	
Test weight 1	0.108557	0.000683	Copper	1.071 kg, at the edge of the table
Test weight 2	0.108546	0.000683	Copper	1.071 kg, at the edge of the table

Table 2 Contributions to momentum of inertia.

The total momentum of inertia is the sum of all contributions

$$J = \sum J_i = 0.269897\,\mathrm{kg\,m^2} \text{ and } \delta J = \sqrt{\sum \delta J_i^2} = 0.000991\,\mathrm{kg\,m^2}. \tag{15}$$

At good vacuum conditions at a pressure $p \le 10^{-4}$ mbar and a constant temperature of $T = 27.5\,^{\circ}\mathrm{C}$ the thrust balance beam has been excited and the free oscillation has been recorded. By the use of FFT analysis the eigen-frequency can be computed which resulted in

$$\omega_0 = 0.953825\,\mathrm{Hz} \text{ and } \delta\omega_0 = 0.002004\,\mathrm{Hz}. \tag{16}$$

With eq. (14) the spring rate of the bearings

$$k = \omega_0^{\,2}\, J = 0.245547\,\mathrm{Nm/rad} \tag{17}$$

can be computed. In addition to that free oscillation above characterization, the same test was performed but the two 1.071 kg weights were replaced with two 3.645 kg weights. With the modified momentum of inertia $J' = 0.791700\,\mathrm{kg\,m^2}$ the modified oscillation frequency of $\omega_0' = 0.584323\,\mathrm{Hz}$ was determined. The modified spring rate $k' = \omega_0'^{\,2}\, J' = 0.270312\,\mathrm{Nm/rad}$ and the dependence of the load was computed to be

$$\frac{k'-k}{m'-m} = 0.004811\,\mathrm{Nm/rad/kg}\,. \tag{18}$$

The mismatch between the thruster weight on the one table and the counter weight on the other one is assumed to be less than 0.1 kg and the corresponding uncertainty is therefore $\delta m = 0.000481\,\mathrm{Nm/rad}$.

In order to determine the influence of the vacuum chamber pressure on the spring rate the free oscillation test was performed at a higher pressure between 0.03 and 2.0 mbar. Due to technical inabilities no constant pressure at this low level could be maintained. The average pressure during recording is therefore $p' = 1.02\,\mathrm{mbar}$ and the slightly modified oscillation frequency of $\omega_0' = 0.954309\,\mathrm{Hz}$ was determined. With the modified spring rate $k' = \omega_0'^{\,2}\, J = 0.245797\,\mathrm{Nm/rad}$ the dependence of the vacuum chamber pressure was computed to be

$$\frac{k'-k}{p'-p} = 0.245122\,\mathrm{Nm/rad/bar}\,. \tag{19}$$

The thruster tests that are performed at FOTEC take only place when the vacuum pressure achieved is below 10^{-4} mbar. The corresponding uncertainty is therefore $\delta v = 2.4512 \times 10^{-8}$ Nm/rad.

If cryo vacuum pumps (ion traps) are to be utilized during the test or if the thruster is expected to heat up, the dependence of the thrust balance temperature on the spring rate of the bearings is required to be investigated. In the following test the thrust balance was heated up to $T' = 52.0\,^{\circ}\mathrm{C}$ and the modified oscillation frequency $\omega_0' = 0.964381\,\mathrm{Hz}$ was determined when thermal equilibrium has been established. The modified spring rate $k' = \omega_0'^{\,2}\, J' = 0.251012\,\mathrm{Nm/rad}$ and the dependence of the temperature was computed to be

$$\frac{k'-k}{T'-T} = 0.000223\,\mathrm{Nm/rad/K}\,. \tag{20}$$

If the maximum temperature change of ±10°C is assumed, the temperature uncertainty contributions on the spring rate results in $\delta T = 2.2308 \times 10^{-3}$ Nm/rad.

Consequently the total uncertainty of the spring rate results in

$$\delta k = \sqrt{\left(\frac{\partial k}{\partial J}\,\delta J\right)^2 + \left(\frac{\partial k}{\partial \omega_0}\,\delta \omega_0\right)^2 + \delta m^2 + \delta v^2 + \delta T^2} = \sqrt{\omega_0{}^4\,\delta J^2 + 4\,\omega_0{}^2\,J^2\,\delta \omega_0{}^2 + \delta m^2 + \delta v^2 + \delta T^2} = 0.002662\,\text{Nm/rad}. \tag{21}$$

When thrusters are characterized at FOTEC the propulsion system is enabled for 60 s. Before and afterwards the deflection of the µN thrust balance is recorded for another 60 s. This not only enables the settling of the desired thrust levels but allows the compensation of the linear drift of the µN thrust balance. For the uncertainty budget calculation that post processing step is not considered and the worst case scenario is considered. With the typical drift rate of 0.8427 nN/s which has been determined in previous tests and with the test duration of 120 s the drift uncertainty results in $\delta d = 0.1011\,\mu$N.

For sake of convenience in section II the angle between the thrust vector and the beam was assumed to be perfectly perpendicular. In eq. (11) the generated force as a function of the spring rate, the distances from the pivot and the deflection is given. For the uncertainty budget calculation the misalignment α of the thruster on the balance needs to be considered and the average thrust becomes to

$$\bar{F} = \frac{k}{r^2 \cos\alpha}\,\bar{x}\,. \tag{22}$$

For the influence of the angle the first order term of error propagation vanished and only second order is considered. The uncertainty is therefore

$$\delta \bar{F} = \sqrt{\left(\frac{\partial \bar{F}}{\partial k}\,\delta k\right)^2 + \left(\frac{\partial \bar{F}}{\partial r}\,\delta r\right)^2 + \left(\frac{\partial \bar{F}}{\partial \bar{x}}\,\delta \bar{x}\right)^2 + \left(\frac{\partial^2 \bar{F}}{\partial \alpha^2}\frac{\alpha^2}{2}\right)^2 + \delta d^2} = \sqrt{\frac{\bar{x}^2}{r^4}\delta k^2 + \frac{4k^2\,\bar{x}^2}{r^6}\delta r^2 + \frac{k^2}{r^4}\delta \bar{x}^2 + \frac{k^2\,\bar{x}^2}{4r^4}\alpha^4 + \delta d^2} \tag{23}$$

In order to avoid the dependency on $\bar{x}$ eq. (11) is utilized once more which results in

$$\delta \bar{F} = \sqrt{\frac{\bar{F}^2}{k^2}\delta k^2 + \frac{k^2}{r^4}\delta \bar{x}^2 + \frac{4\bar{F}^2}{r^2}\delta r^2 + \frac{\bar{F}^2}{4}\alpha^2 + \delta d^2} = \sqrt{8.535 \times 10^{-12} + 1.651 \times 10^{-4}\,\bar{F}^2}\,. \tag{24}$$

with the spring rate from eq. (17), its uncertainty from eq. (21), the distance from the pivot $r = 0.29\,\text{m}$, the corresponding positioning inaccuracy $\delta r = 0.001\,\text{m}$, the assumed misalignment of $\alpha = 1° = 0.01745\,\text{rad}$ and the uncertainty of the optical displacement transducer $\delta \bar{x} = 1.0 \times 10^{-6}\,\text{m}$. In Fig. 6 the uncertainty as a function of the thrust is shown (coverage factor 1).

For low thrust levels the minimum uncertainty is 2.92 µN and the prevailing factor is the uncertainty of the optical displacement transducer. Whereas at high thrust levels the spring rate uncertainty becomes the crucial factor which is limiting measurement accuracy.

For future configurations the force actuator mentioned in section IV shall be developed and utilized. In force-feedback operation the beam of the µN thrust balance is actively held in resting position by balancing the generated force by the thruster with the force actuator F_a

$$\tau = F_a\,r_a = \bar{F}\,r\cos\alpha \tag{25}$$

with the force actuator spaced from the pivot by r_a. Note that though $r_a = r$ and $F_a = \bar{F}$ will be used in practice for the sake of the uncertainty budget calculation this notation is utilized. With the utilization of the force actuator neither the spring rate nor the absolute accuracy of the optical displacement transducer does affect the measurement of the thrust anymore. Regarding Table 1, most of the contributions to the total uncertainty budget vanish – only the drift rate δd, the distance to the pivot δr and the pointing inaccuracy of thruster mounting α persist. The force actuator can be calibrated by the use of scale under vacuum and the uncertainty is assumed being proportional to the generated thrust and will be denoted as δa.

The total uncertainty budget therefore results in

$$\delta\bar{F} = \sqrt{\frac{2\bar{F}^2}{r^2}\delta r^2 + \frac{\bar{F}^2}{4}\alpha^2 + \delta d^2 + \delta a^2}\,. \tag{26}$$

For various force actuator uncertainty levels 0.1%, 0.5% and 1.0% of nominal thrust the total uncertainty budget is illustrated in Fig. 6 in addition to the one in deflection operation mode. One can immediately recognize the reduced uncertainty particularly at low level thrust measurements. It is notable that at low force measurements the actuator uncertainty $\delta a \le 10^{-3} \times F_a$ predominates over the other factors of eq. (26).

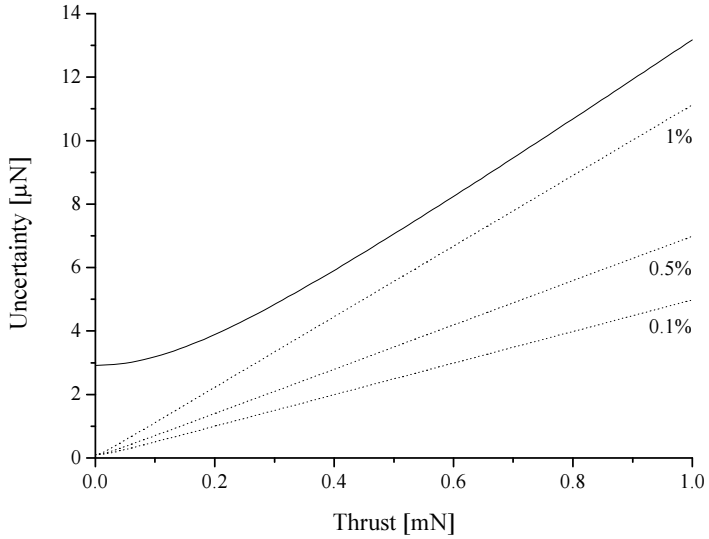

Fig. 6 Thrust measurement uncertainty for thrust levels up to 1 mN (solid line), force-feedback mode with force actuator operation at various uncertainty levels (dashed lines)

VI. Outlook and Conclusions

For the characterization and thrust measurement of electric propulsion systems a torsion-based µN thrust balance was developed. Due to the utilization of spring bearings the maximum load on each table is up to 13 kg whereas the spring rate is comparatively low which allows high sensitivity and low noise measurements.

In order to supply the electric thruster and to control or monitor it during operation special liquid metal-based electrical feed-throughs contacts were developed. No influence on the spring rate which might be caused by cables or other phantom forces could be observed even at high voltage or current levels.

For the calibration of the thrust measurement system and thus the determination of the spring rate of the bearings the eigen-frequency is measured during free oscillation. Knowing the total momentum of inertia the spring rate and the thrust-to-deflection ratio can directly be calculated.

For the determination of the uncertainty budget the uncertainties during calibration and the positioning inaccuracy of the thruster, the drift rate of the µN thrust balance, the temperature influence, the vacuum pressure influence and the absolute accuracy of the optical displacement sensor were considered.

Within the scope of a test campaign the µN thrust balance was tested with a cold gas thruster at the ESA propulsion laboratory at ESTEC. The acquired tests data are still to be evaluated and the test results will be published thereafter.

In addition the utilization of a force actuator during calibration or thruster operation (force-feedback mode) was proposed for future extension. The expected uncertainty could strongly be reduced since major contributions to the total uncertainty budget like the uncertainty of the spring rate or the optical displacement sensor would vanish. If the µN thrust balance is operated in force-feedback mode the passive damping system is not required anymore and the active control loop will keep the beam in resting position which will also help to increase the response frequency of the system.

References

[1] K. Marhold, M. Tajmar, *Micronewton Thrust Balance for Indium FEEP Thrusters*, 41st Joint Propulsion Conference, AIAA-2005-4387

[2] N. Buldrini, M. Tajmar, K. Marhold, B. Seifert, *Experimental Results of the Woodward Effect on a µN Thrust Balance*, STAIF Conference, 2006

[3] D. Krejci, B. Seifert, *Miniaturized pulsed plasma thrusters for CubeSats: modeling and direct thrust measurement*, 61st International Astronautical Congress, 2010

[4] A. Reissner, N. Buldrini, B. Seifert, F. Plesescu, C. Scharlemann, J. Gonzales del Amo, *mN-FEEP thruster module design and preliminary performance testing*, 33rd International Electric Propulsion Conference, 2013

[5] A. Pancotti, T. Lilly, A. Ketsdever, V. Aguero, P. Schwoebel, *Development of a Thrust Stand Micro-Balance to Assess Micropropulsion Performance*, 41st Joint Propulsion Conference, AIAA-2005-4415, 2005

[6] D. Krejci, B. Seifert, C. Scharlemann, *Endurance testing of a pulsed plasma thruster for nano-satellites*, Acta Astronautica Vol. 91, p. 187-193, 2013

[7] B. D´Souza, A. Ketsdever, *Development of a Nano-Impulse Balance for Micropropulsion Systems*, 1st AIAA/ASME/SAE/ASEE Joint Propulsion Conference, AIAA-2005-4080, 2005

[8] M. Camero-Castaño, *A torsional balance for the characterization of microNewton thrusters*, Review of scientific Instruments, Vol. 74-10, 2003

[9] J. Woodward, *Making Starships and Stargates: The Science of Interstellar Transport and Absurdly Benign Wormholes*, p. 136, Springer Praxis Books, NYC: Springer Publishing, 2012

[10] M. Gamero-Castaño, V. Hruby, M. Martínez-Sánchez, *A Torsional Balance that Resolves Sub-micro-Newton Forces*, International Electric Propulsion Conference, 01-235

[11] N. Selden, A. Ketsdevera, *Comparison of force balance calibration techniques for the nano-Newton range*, Review of Scientific Instruments, Vol. 74/12